Experimental study of geysers through a vent pipe connected to flowing sewers

Biao Huang, Shiqiang Wu, David Z. Zhu and Harry E. Schulz

ABSTRACT

Geysers of air–water mixtures in urban drainage systems is receiving considerable attention due to public safety concerns. However, the geyser formation process and its relation with air release from pressurized pipes are still relatively little known. A large-scale physical model, that consisted of a main tunnel with a diameter of 270 mm and a length of 25 m connecting two reservoirs and a vertical vent pipe, was established to investigate geyser evolution and pressure transients. Experimental results including dynamic pressure data and high speed videos were analysed in order to characterize geysering flow through the vent pipe. Pressure transients were observed during geysering events. Their amplitudes were found to be about three times the driving pressure head and their periods were close to the classic surge tank predictions. The influence of flow rate and vent pipe size were examined: geyser heights and pressure peaks decreased for small flow rate and large diameter vent pipe. It is suggested that geyser heights are related with the pressure head and the density of the air–water mixture.

Key words | air–water flow, geysering, hydraulic transient, sewer, vent pipe

Biao Huang
Smart Cities Research Institute,
Zhengzhou University,
Zhengzhou 450001,
China

Biao Huang
Shiqiang Wu (corresponding author)
State Key Laboratory of Hydrology-Water Resources and Hydraulic Engineering,
Nanjing Hydraulic Research Institute,
Nanjing 210029,
China
E-mail: *sqwu@nhri.cn*

Biao Huang
David Z. Zhu
Harry E. Schulz
Department of Civil and Environmental Engineering,
University of Alberta,
Edmonton, Alberta T6G 2W2,
Canada

Harry E. Schulz
School of Engineering at São Carlos,
University of São Paulo,
São Carlos, 13566-590,
Brazil

INTRODUCTION

Geysering phenomena is commonly observed in drainage systems when subjected to intense rain storms (Guo & Song 1990; Wright *et al.* 2010, and Hager 2012, among others). Geysering occurrence is often related with flow transitions, air entrapment and its release from pressurized flow. For actual drainage tunnels, flow transition from gravity flow to pressurized flow may occur when the upstream influx is suddenly increased and/or the outflow is reduced considerably. Air entrapment can occur due to surcharge flow, especially when downstream ventilation condition is unfavourable, and the entrapped air pocket may be compressed continuously during this process. When the air pocket reaches ventilation structures like a vent tower or a dropshaft, it moves upward and may push water out, forming geysers. The physical process of geysering induced by air release through water-filled vertical shaft was conceptually described by Wright *et al.* (2011). Pressure transients during such process were found to be the main cause for structure failure (Hamam & McCorquodale 1982; Zhou *et al.* 2002; Pozos-Estrada *et al.* 2015), excessive surges (Song *et al.* 1983) and water overshooting through the vertical shaft (Wright *et al.* 2010).

The air–water flow in vertical pipe has been widely studied, including rising bubbles and release of large air pockets. The terminal velocity of a rising air bubble was given by Davies & Taylor (1950), as $0.35\sqrt{gd}$ where g is gravity acceleration and d the diameter of the pipe. It should have a spherical cap (front) and an open unsteady wake (rear), experimentally observed by Bhaga & Weber (1981). For the condition with large air pockets, the water column undergoes mass loss due to a counter-current water film that forms around the pipe wall, which leads to an upwards acceleration of the water parcel, inducing the occurrence of geysering (Vasconcelos & Wright 2011). Wright *et al.* (2011) assumed that geysering processes in actual drainage systems may involve film flow and flooding instability.

The influences of entrapped air and its release in sewer systems have been studied. Large pressure oscillations were

doi: 10.2166/wst.2018.085

reported, e.g. Martin (1976), Zhou *et al.* (2002), and Wright *et al.* (2010). Ferreri *et al.* (2014) attributed these pressure transients to the pulsations of air pockets during their migration-release processes. The effects of entrapped air pocket volume, driving head, air-vent size and water compressibility have been studied experimentally and numerically for horizontal and/or slope pipes (Zhou *et al.* 2002, 2011; Martin & Lee 2012). In addition to the influence of entrapped air pocket in sewer trunks, cushion effects and water slamming were found when air–water interactions existed in vertical pipes (Lingireddy *et al.* 2004; Fontana *et al.* 2016). Pressure patterns induced by air release from a pressurized system were found to be similar with water hammer waves, whereas the amplitude of low-frequency pressure oscillation induced by air release tends to be lower than pressure spikes of water hammer (Li & McCorquodale 1999; De Martino *et al.* 2008).

Experiments performed by Lewis (2011) revealed several key characteristics of geysering phenomena, including air–water interface movements. Wright *et al.* (2010) pointed out that the observed geyser height should be controlled by the density of air–water mixture since the measured dynamic pressure during geyser events was not able to lift water to the measured heights. However, the interplay of pressure spikes and the production of air–water mixture is still poorly understood. Vasconcelos & Wright (2011) and Lewis (2011) proposed models to calculate the movement of air–water interface and free surface. However, geyser heights were not considered in these models, and the corresponding prediction using the final velocity of the interface was not close to those observations in experiments and field studies (Lewis 2011).

Despite the above advancements, it is still unclear about the relationship between flow conditions and geyser intensity. Pressure transients during air release also need to be analysed further in order to protect public safety. A large-scale physical model was built to observe, with the aid of a high speed camera, geysering flow evolution in a vented stormwater system and geyser types that are associated with different driving conditions. Pressure data were recorded to characterize the surge amplitude and frequency, and the relationship between pressure peaks and geyser heights was then examined. This study also seeks to explore different relevant variables that influence geysering flow, including initial and final flow rates, and the diameter and length of the vertical pipe.

EXPERIMENTAL PROGRAM

A large-scale physical model was constructed in the Nanjing Hydraulic Research Institute, China, to investigate geysering through a vertical riser. The model as shown in Figure 1 consisted of two circular plexiglas pipes with a diameter of D = 0.27 m. The 2% sloped pipe had a length of 17 m, and the horizontal pipe, 8 m. The vent pipe was placed at 13.4 m downstream of the inlet. Upstream and downstream reservoirs had the dimensions of 4 m × 2.5 m × 2.5 m (length by width by height) and 2.25 m × 2.0 m × 1.08 m, respectively. A gate was placed at the end wall of the downstream tank to drain the water and/or adjust the water level. A pressure transducer (PT) with an accuracy of 1% of the range was installed upstream of the vent pipe at pipe invert, shown as PT in Figure 1. The inflow rate was measured using an ultrasonic flow meter (TUF-2000BNB, from Baoji HQsensor Company, China) with an accuracy of 1%. All the experiments were recorded by digital cameras (Nikon D5300 and Nikon D90, Phantom v663 from Shanghai Noncon Company, China and iPhone 6) and two 1 KW lamps were used to enhance the light field when utilising high speed video cameras at 240 frames per second (Phantom v663 and iPhone 6). Digital image processing methods were employed to analyse the movement and interaction of the air–water interface. Pressure data were denoised and validated with those obtained from manometer tubes. For pressure data processing, the wavelet packet threshold denoising method (MATLAB 2015) was adopted to filter out background noises and the initial hydrostatic pressure was also subtracted in the analysis.

The experiments were started by first generating an initial steady flow in the main tunnel with a flow rate Q_0. Then the inflow from the upstream reservoir was increased by opening the control valve quickly (less than 1 s) to a final flow rate Q_1. In the meantime, the gate of the downstream reservoir was shut down, which resulted in changing flow conditions both upstream and downstream. Consequently, air was trapped in the system. The sequence of events including air entrapment, compression and release was then observed and registered, as sketched in Figure 2. After the air exhaustion, full pipe flow was observed and maintained for 30 s. A total of 22 laboratory tests on geyser formation have been performed with the initial flow rates 20–60 L/s, corresponding to different locations of hydraulic jump, and the typical final flow rates 77–122 L/s. A summary of flow conditions and parameters is given in Table 1. The scenarios indicated as Exp. A allowed studying the effects of the initial flow rate Q_0 by varying it from 0.1686–0.5057 with a constant final flow rate $Q_1 = 0.6490$ and for a vent pipe with a diameter $d = 40$ mm and a length $L_s = 1$ m. In this study, the flow rates were non-dimensionalized as $Q/\sqrt{gD^5}$ where Q is the flow rate,

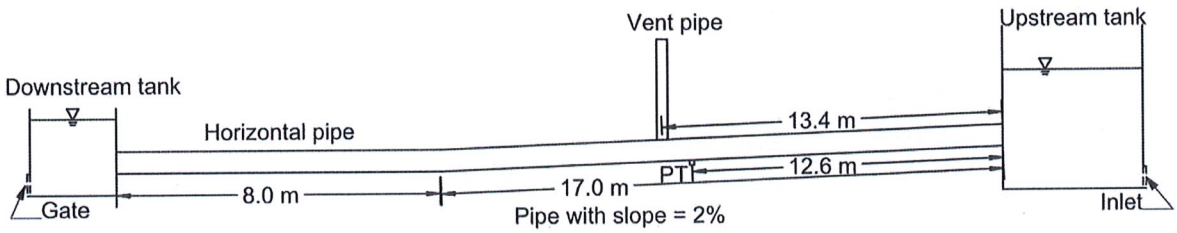

Figure 1 | Schematic diagram of experimental setup (not to scale; PT: pressure transducer).

g the gravity acceleration and D the diameter of the main tunnel. The scenarios indicated by Exp. B have similar conditions as Exp. A, with the exception of $Q_1 = 0.9103$, used to verify the effect of Q_1 on the previous Q_0 conditions. Exp. A and B were performed to observe geyser formation and its dependence on the different flow rates. Exp. C considers a constant initial flow rate $Q_0 = 0.3371$ and a range of $Q_1 = 0.6827$–1.0283, scenarios that allowed studying the relationship between pressure transients and final flow rate. The effect of the vent pipe with a larger diameter ($d = 60$ mm) and a longer length ($L_s = 2$ m) were studied in Exp. D and Exp. E, respectively.

RESULTS AND DISCUSSION

Experimental observations

The experimental procedures and flow evolution are described as follows and sketched in Figure 2:

1. Initial steady state stage: As shown in Figure 2(a), the inflow rate Q_0 was set equal to the outflow rate. Inlet-control culvert flow was observed in the system, with the supercritical flow in the part of the inclined pipe upstream of the hydraulic jump, and full pipe flow downstream of the hydraulic jump. Both the inlet and outlet were submerged, and air was provided by the vertical vent pipe. The air flow entering through the vent pipe was equal to that carried downstream of the hydraulic jump, thus the location of the jump remained stationary. For all the runs, the initial steady flow was maintained for about 60 s, during which measurements were taken, including hydraulic parameters, pressure variations and videos.
2. Pipe filling phase: The initial inflow rate Q_0 of the upstream inlet was increased to Q_1. Meanwhile, the gate in the downstream reservoir was closed immediately. The backwater surge, i.e. the moving hydraulic jump, moved upstream due to the rise of the downstream water level and the increased flow rate, resulting in an abrupt change of surface level, i.e. pipe pressurization. The surge front consisted of a tilted foamy interface, with strong turbulence. As the surge moved upstream, the air within the main pipe was partially pushed out through the vent pipe (Figure 2(b)).
3. Air entrapment and compression: After the surge, front moved pass the vent pipe, the remaining air was entrapped due to the seal effect of the air–water mixture at the bottom of the vent pipe (Figure 2(c)). The surge then moved much more slowly and the entrapped air was undergoing a compression process. The upstream air could only be removed via the hydraulic jump at this stage and the air pockets formed downstream of the vent pipe were carried away by the flow.
4. Air removal: The air could entrain into the hydraulic jump and be carried downstream, but its amount was relatively small. Air expulsion through the vent pipe (Figure 2(d)), usually producing geysers, accounted for the most air removal.
5. Full pipe flow: Following the air removal, full pipe flow was observed in the system, as shown in Figure 2(e). At this stage, recorded pressure data remained steady and constant.

The laboratory observations revealed several mechanisms of geyser formation: geysers can be basically grouped into three types, namely short column jets, column-breaking jets and spray-like jets according to flow characteristics. Geysers in the form of short column jet and column-breaking jet are illustrated in Figure 3. Generally, prior to the air release, a water column existed in the vent pipe. When the pressurized air pocket arrived at the vertical pipe, it ascended along the pipe and pushed the short water column upwards (Figure 3(a) and 3(b)). The overtopping then occurred since air continually moved upward, as shown in Figure 3(c). Water column overshooting could be observed (Figure 3(d)), which suggested the name of such geysers as short column jets. For the release of air pockets with a medium or large volume, short column jet geysers

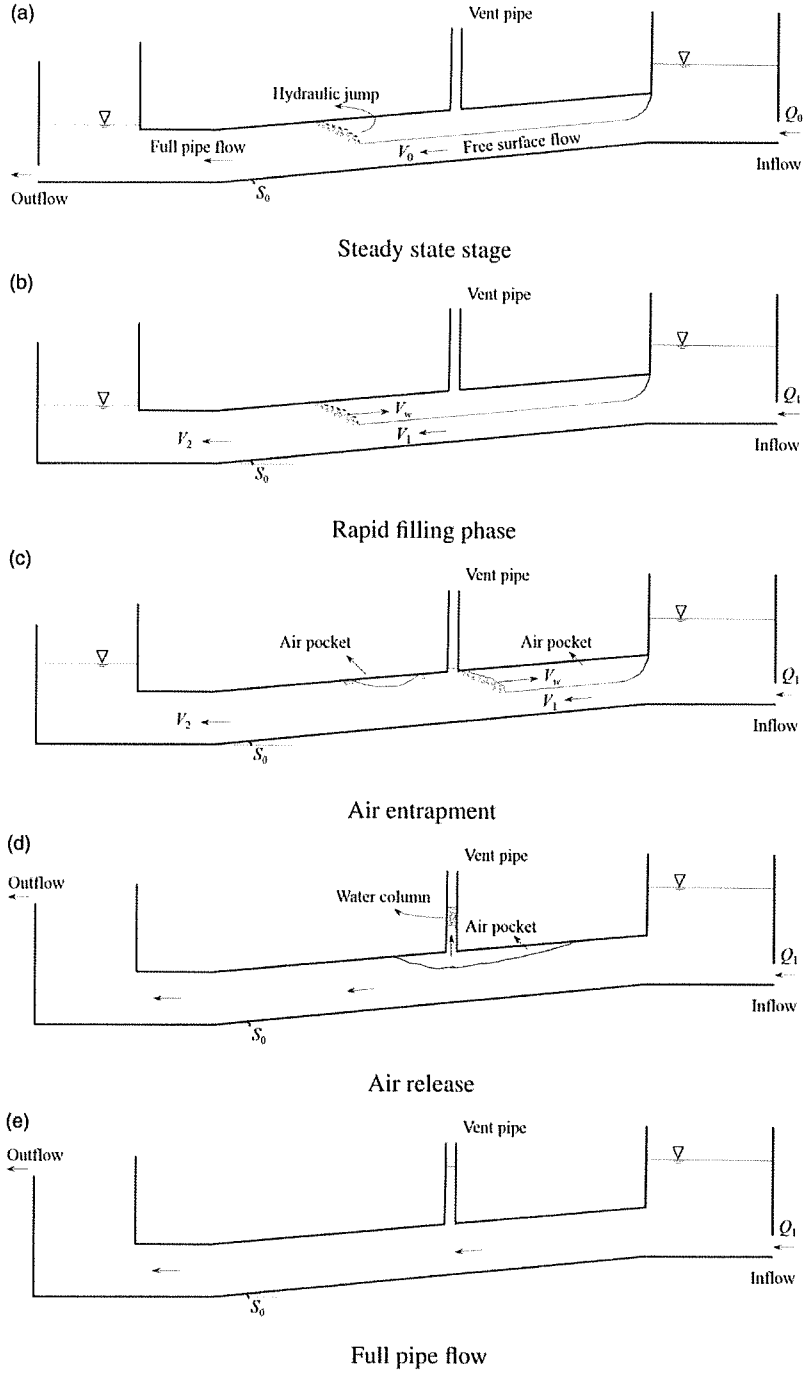

Figure 2 | Geysering flow evolution.

are very common. During the geysering and/or air release process, downwards flow films were considered to be important before the ejection of water. The final velocity and height of short column jets depend on the mass loss due to overshooting, but before this final stage, downwards films may affect the acceleration of the column.

After the geyser event of a short column jet, the air-water interface breaks and the air pocket connects with

Table 1 | Experimental scenarios

Exp.	Vent pipe diameter d(mm)	Vent pipe length L_s(m)	Initial flow rate Q_0	Final flow rate Q_1
A	40	1.0	0.1686; 0.2529; 0.3371; 0.4214; 0.5057	0.6490
B	40	1.0	0.1686; 0.2529; 0.3371; 0.4214; 0.5057	0.9103
C	40	1.0	0.3371	0.6827; 0.7080; 0.8176; 0.8681; 0.9100; 1.0283
D	60	1.0	0.1686; 0.3371; 0.5057	0.9103
E	40	2.0	0.1686; 0.3371; 0.5057	0.9103

Note: Flow rate Q_0 and Q_1 are non-dimensionalized using $Q/\sqrt{gD^5}$ where Q is the flow rate, g the gravity acceleration and D the diameter of the main tunnel.

the atmosphere. The pressure relief within the air pocket can induce the acceleration of the water in the main tunnel toward the base of the vent pipe, leading to choking or slamming phenomena, as shown in Figure 3(e). The water surge leads to overshooting, and column-breaking geysers result in this way. A notable feature for this type is that the fluid in the vent pipe exists in a fashion of breaking water column (Figure 3(f) and 3(g)). Because of the intermittency of the contact between air pocket and vent pipe, the air release can be interrupted and the remaining

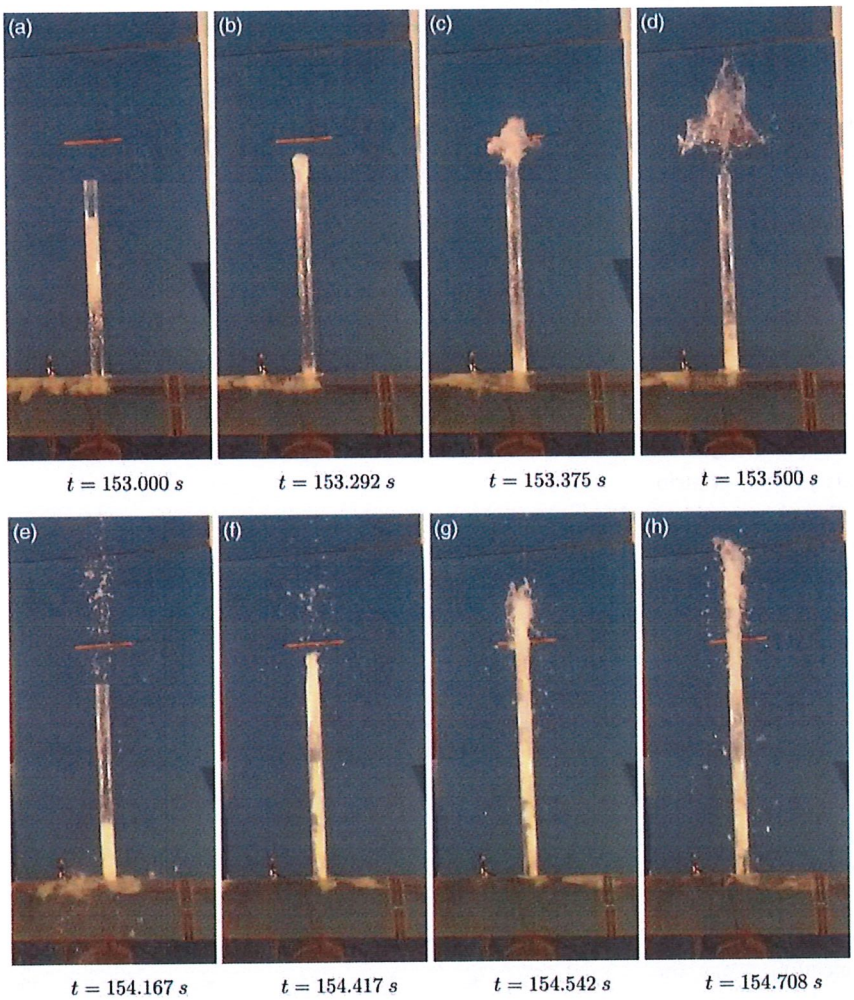

Figure 3 | Observations of geyser events through the vent pipe (Exp. D with $Q_0 = 0.3371$): short column jet (a)–(d); column-breaking jet (e)–(h); note that the flow direction is from right to left.

air pocket may be subjected to a short compression course before generating another geyser. A compressed air pocket in the main tunnel from the upstream can be clearly seen in Figure 3(h), which should be released later. Thus, large air pockets in the main tunnel can generate a series of geysers because of the repetitive process described here. Such serial geysers can be seen in videos of actual drainage systems (Wright *et al.* 2011). Compared to short column jet geysers, such geysers were mainly caused by inertia surge and air effects. Therefore, pressure transients should contribute to geyser intensity. Our experimental results suggest that the geyser height of column-breaking jets is larger than that of short column geysers for most tests. Figure 3(d) and 3(h) allow a first qualitative comparison between the mentioned heights.

In addition to the two types of geysers described above, spray-like geysers were also observed in our experiments, which were partially attributed to complicated air–water interactions and film flow reversal or flooding (refer to Figure S1 in supplementary material, available with the online version of this paper). Flooding is observed when the fluid in a downward flow changes direction, which is initiated when the liquid velocity in the film at the interface changes direction (Hanratty 2013). The air–water interfacial stress and pressure gradient supply the motive forces pulling the film upward as a consequence of air release. When a large volume of air (large air pocket) was released, the velocity of the escaping air may be two orders of magnitude greater than that of the water flow. This may be due to the pressure difference between the compressed air pocket and the outer environment, which is capable of introducing flooding and entraining water drops. This possibly contributes to the spray-like geysers.

Three mechanisms were considered to be responsible for the geyser types discussed above: (1) for short column jets, the short liquid column within the vent pipe is accelerated by the imposed head (air pressure), and can overshoot; (2) for column-breaking jets, pressure surge induced by air release can result in eruption of water or air-water mixture; (3) for spray-like jets, the drive head is capable of raising well-mixed air-water mixture, analogous to airlift pumping in some sense. The first mechanism seems to be occurring for low remaining mass in the vertical tube, and for short times. The second mechanism is likely to allow higher velocities and also the maintenance of geysering while the system is pressurized. The third allows a long period ejection, while the required conditions are maintained, which may conduce much larger velocities and heights.

Pressure characteristics

The pressure pattern for a typical case (Exp. D with $Q_0 = 0.3371$) is shown in Figure 4. Initial hydrostatic pressure was subtracted and the steady flow stage can be clearly seen at the beginning. The pressure started to increase when the filling process began. However, the large pressure oscillations started at about 180 s when the air pocket moved to the vent pipe and geysers formed by air release through the vent pipe. The oscillations ended at about 270 s after all the air was expelled out of the system. The pressure then remained constant, and the flow became full pipe flow. Note that the pulsation of entrapped air does not show considerable pressure fluctuations, compared to air release. The pressure pattern shown in Figure 4 includes all the stages of the flow evolution in the experiment.

The pressure oscillation corresponds to a series of geyser events in laboratory tests (Figure 5). Geysers were accompanied by a remarkable pressure peak at the beginning and significant fluctuations soon afterwards, as shown in the pressure patterns. For the cases with $Q_1 = 0.6490$ but various Q_0 (Exp. A), the ranges of the oscillation period are 0.49–1.33 s, 0.76–1.36 s, 0.43–1.04 s and 0.42–1.27 s as shown in Figure 5(a). For the cases with $Q_0 = 0.3371$ but various Q_1 (Exp. C), these ranges are 0.4–1.3 s, 0.4–1.0 s, 0.4–0.9 s, 0.4–0.8 s, 0.4–0.7 s, and 0.3–0.8 s as shown in Figure 5(b). The range of such periods is thus about 0.3–1.36 s according to all the tests. A notable feature of pressure oscillations is that one geyser event

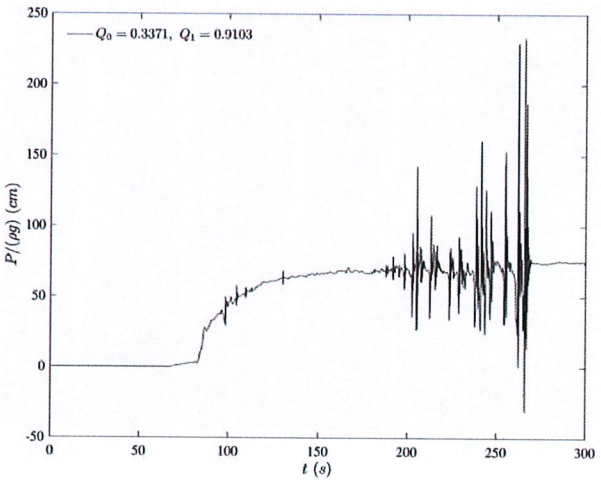

Figure 4 | Pressure diagram for a typical run (Exp. D with $Q_0 = 0.3371$).

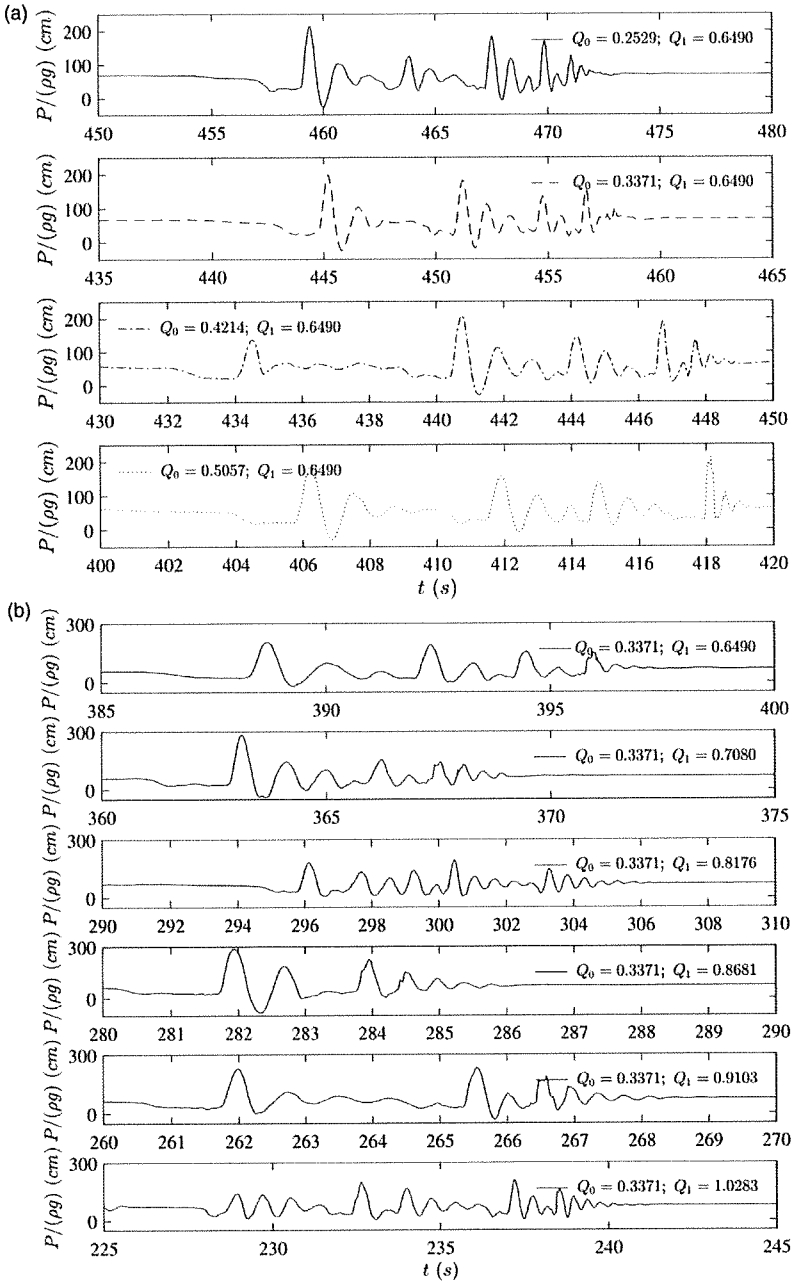

Figure 5 | Pressure transients due to air release for: (a) Exp. A; (b) Exp. C.

corresponds to a peak following by its damped waves, and the sequence of peaks and waves presents a slightly different magnitude of period. Note that the maximum pressure value is about three to four times the driving average pressure. Thus, the pressure peak induced by air release is much less than those produced by waterhammer, which can be 10 or even 100 times of the drive head.

Considering the vertical vent pipe as similar to a surge tank, a comparison between measured and predicted pressure peaks and periods of oscillation was performed. The oscillation period T_w and the pressure magnitude B_1

for a surge tank can be calculated as follows (Wylie & Streeter 1978), neglecting friction and considering instantaneous downstream closure,

$$T_w = 2\pi\sqrt{\frac{L_T A_s}{gA_T}}$$

$$B_1 = \frac{Q_{1D}}{A_s}\sqrt{\frac{L_T A_s}{gA_T}}$$

where A_T and L_T are the area and length of the main tunnel, respectively, A_s is the area of the surge tank (vent pipe in the present study), and Q_{1D} is the flow rate Q_1 with the dimension of m^3/s. For the laboratory tests shown in Figure 5, $L_T = 12.6$ m, $A_T = 0.0573$ m^2, $A_s = 0.0013$ m^2, and $Q_{1D} = 0.077$ m^3/s for $Q_1 = 0.6490$. Thus, the cycle of the fluctuation T_w calculated by the equation given above is equal to 1.04 s, which is in the range of 0.3–1.36 s observed in the experiments, furnishing a way to infer approximately the magnitude of the periods of oscillations. However, the calculated pressure magnitude is about 10.2 m, much larger than the measurements of around 2.1 m. It must be remembered that the surge tank equations consider full section water flows, so that no air exists to be compressed as sketched in Figure 2(c). Having no compression effects of entrapped air pockets, higher pressure peaks are expected when using the mentioned surge tank equations. Results from Li & McCorquodale (1999) and De Martino *et al.* (2008) indicate that waterhammer pressure transients have larger peaks than those induced by air release, which also points to the adequacy of our results. Note that the air–water interplay can play a significant role and lead to more intense geysers in much larger stormwater tunnels.

Influence of flow rate, vent pipe diameter and length

For identical initial flow rates, the occurrence of large final flow rates is expected to generate high water levels upstream and downstream, resulting in pressure increases for the trapped air, which, in turn, can cause severe surge transients. Figure 6(a) shows pressure peaks measured during the geysering process for different Q_0 and Q_1 in Exp. A and B. The results imply that a larger Q_1 can, in fact, induce more severe pressure transients for the two Q_1 values tested in our experiments. This possibility is discussed in more details later with geyser heights, where a number of Q_1 values is presented. Considering Q_0, the amplitude of the pressure peaks shown in Figure 6(a) is firstly reduced for increasing Q_0. In the sequence, the amplitude of the pressure peaks increases for further increasing in Q_0. The present experimental conditions produced minima for the pressure peaks in relation to Q_0 for both values used for Q_1. In the observation of Ferreri *et al.* (2014), the amplitude of high oscillations climbs and then declines as the flow rate increases, which suggests that experimental conditions may have influence on the results.

Figure 6(b) shows the measured peak pressure for the vent pipes of length $L_s = 1.0$ and 2.0 m in Exp. B and E. The peak pressure is plotted against the initial flow rate Q_0, and shows to be larger for the shorter vent pipe. Only three peak values for the vent pipe with $L_s = 2.0$ m were measured, so that it is difficult to suggest evident average

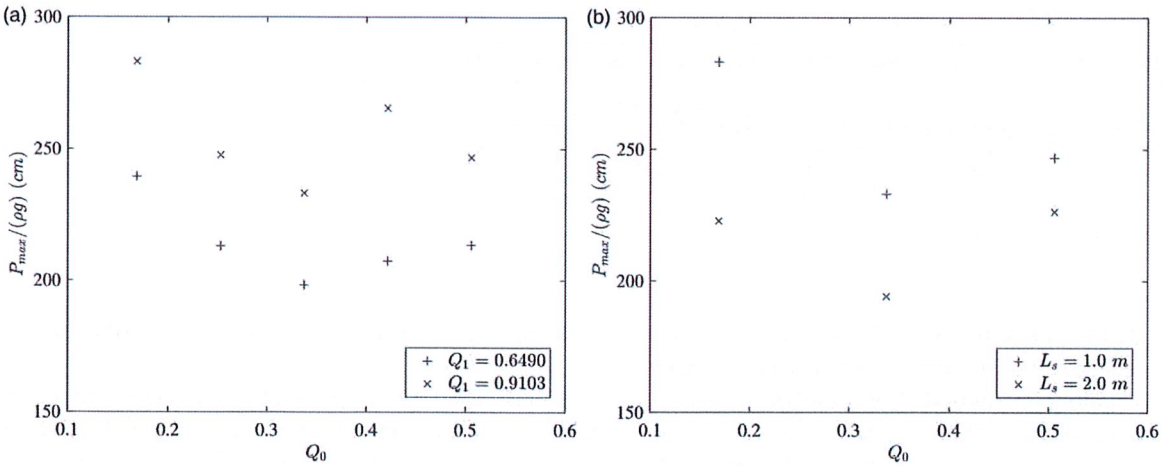

Figure 6 | Comparison of pressure peaks for: (a) different final flow rates; (b) different vent pipe lengths.

trends. However, the results of the 2.0 m long vent pipe reveal that the peak pressure for geysering decreases notably, when compared to the 1.0 m pipe, particularly for the cases with small initial flow rate.

The diameter of the vent pipe influences the geyser height (of the column-breaking jets), and Figure 7 shows that a larger vent pipe reduces both the peak pressure and the geyser height (indicated as H_g), which confirms earlier findings by Lewis (2011). Film flow for a larger diameter vent pipe may be responsible for the reduction, as stated by Vasconcelos & Wright (2011). For large initial flow rates Q_0, it can be seen that the geyser intensity (pressure and height) decreases less when increasing d, which may imply a significant role of the imposed flow increment (Q_1-Q_0). The data also suggest that the maximum pressure values are comparable to those in Exp. A, with the order of about three times of the driving pressure head H. The non-dimensionalized geyser heights show the relative magnitude order of the geyser heights under the conditions of the present set of experiments, furnishing larger results than those reported by Lewis (2011), who worked only with water surge, without the presence of air-water interactions. It is also noted that the geyser height is about two times of the peak pressure, likely implying that the water content of the jet is about a half which seems convincible according to our experimental images.

The peak values of the pressure heads during geysering process and the related geyser heights of column-breaking jets observed in the experiments are shown in Figure 8. When considering the data of Figure 6(a), the mean peak pressure heads are 214 cm and 255 cm for $Q_1 = 0.6149$ and 0.9103, respectively. In Figure 8, however, these mean values, represented by the solid and dashed lines, are encompassed by the general fluctuation of the peak pressures. So, no evident mean trends are observed in this more detailed analysis. A possible explanation is that the geyser formation is subjected to various parameters, such as geometry and air volume, which also affect the pressure evolution. The average geyser heights shown in Figure 8 are about two times as large as the peak pressure head, indicating that only the information obtained from the pressure transients is not sufficient for predicting accurately geyser heights (H_g). This also suggests incorporating the mixture density. It is worth mentioning that geysers (column breaking jets) attain higher heights when ejecting well-mixed air–water flows, as is common in observed geysers. This is consistent with our video images. Therefore, not only the pressure head but also the density of the jets shooting out influence the geyser height significantly.

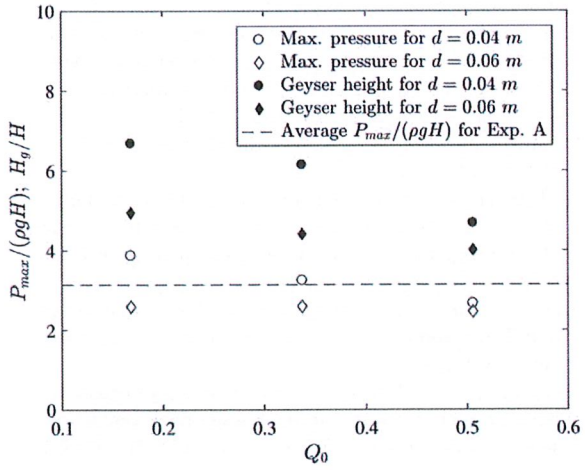

Figure 7 | Comparisons of pressure peaks P_{max} and geyser heights H_g between vent pipes with different diameter (Exp. B and D, both with $Q_1 = 0.9103$) and the average of maximum pressure for Exp. A with $Q_1 = 0.6490$ (H = the driving head).

CONCLUSIONS

In drainage systems with vent pipes, geysering may occur during transient process from free surface flow to pressurized flow. A large-scale laboratory model, which can trap air pockets of large volume through changing flow conditions, was implemented to study air-water interactions and pressure signatures over the geysering evolution. Detailed information of geysers of different types was obtained. A group of parameters including main geometrical information of the setup, initial and final flow rates, and the specific geometrical information of the vent pipe, like its

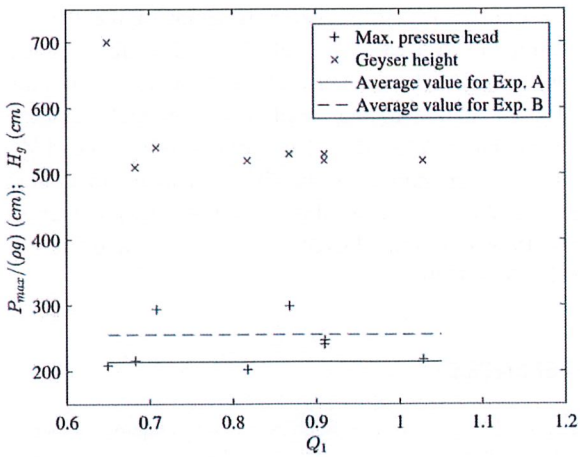

Figure 8 | Peak pressure values and maximum geyser heights as a function of Q_1 for Exp. C.

length and diameter were used to examine the geyser characteristics.

For the present experimental conditions, three main types of geysering were observed: short column jets, column-breaking jets and spray-like jets. It follows that geysering in drainage systems may occur following different mechanisms briefly reported in this study. Pressure measurements of all the experimental runs were analysed and associated with the air release process, which imply that air release during geyser events can generate pressure oscillations, with the order of magnitude of their periods comparable to that computed from classic surge tank theory. Pressure peaks are three to four times the driving pressure head, yet much smaller than those induced by waterhammer. Our experiments also showed a consistent reduction of the periods during oscillations. These results point to the fact that pressure oscillations of geysering flows present particularities on periods and magnitudes that need further investigation.

Experimental results suggest that the vent pipe with larger diameter can generally reduce pressure peaks and geyser heights. The observed average geyser height was about two times as large as the pressure head peak value, which suggests to incorporate the air–water mixture density in the analysis. However, the complicated interactions among air, water and pipe walls (observed in the films) still introduce difficulties to adequately evaluate the density of the mixtures, indicating the need of further investigation.

ACKNOWLEDGEMENTS

This work is partially sponsored by National Natural Science Foundation of China (Grant No. 51379128), the Major Consulting and Research Program of the Chinese Academy of Engineering (2015-ZD-07-01-02), Central Public-Interest Scientific Institution Basal Research Fund (Y116022) and Nanjing Hydraulic Research Institute Research Fund (Y116017). The authors also acknowledge the financial support from the China Scholarship Council (CSC No. 201508320238), the Natural Sciences and Engineering Research Council (NSERC) of Canada, and CAPES/Brazil (5723/15/9).

REFERENCES

Bhaga, D. & Weber, M. 1981 Bubbles in viscous liquids: shapes, wakes and velocities. *Journal of Fluid Mechanics* **105**, 61–85.

Davies, R. & Taylor, G. 1950 The mechanics of large bubbles rising through extended liquids and through liquids in tubes. In: *Proceedings of the Royal Society of London A: Mathematical, Physical and Engineering Sciences*, The Royal Society, pp. 375–390.

De Martino, G., Fontana, N. & Giugni, M. 2008 Transient flow caused by air expulsion through an orifice. *Journal of Hydraulic Engineering* **134** (9), 1395–1399.

Ferreri, G. B., Ciraolo, G. & Lo Re, C. 2014 Storm sewer pressurization transient–an experimental investigation. *Journal of Hydraulic Research* **52** (5), 666–675.

Fontana, N., Galdiero, E. & Giugni, M. 2016 Pressure surges caused by air release in water pipelines. *Journal of Hydraulic Research* **54** (4), 461–472.

Guo, Q. & Song, C. C. 1990 Surging in urban storm drainage systems. *Journal of Hydraulic Engineering* **116** (12), 1523–1537.

Hager, W. H. 2012 Environmental aspects of wastewater hydraulics. In: *Environmental Fluid Mechanics: Memorial Volume in Honour of Prof. Gerhard H. Jirka,* Edited by Wolfgang Rodi, Markus Uhlmann. CRC Press, Boca Raton, FL, USA, pp. 249.

Hamam, M. & McCorquodale, J. 1982 Transient conditions in the transition from gravity to surcharged sewer flow. *Canadian Journal of Civil Engineering* **9** (2), 189–196.

Hanratty, T. J. 2013 *Physics of Gas-Liquid Flows.* Cambridge University Press, New York, NY, USA.

Lewis, J. W. 2011 *A Physical Investigation of Air/Water Interactions Leading to Geyser Events in Rapid Filling Pipelines.* PhD Thesis, University of Michigan, Ann Arbor, MI, USA.

Li, J. & McCorquodale, A. 1999 Modeling mixed flow in storm sewers. *Journal of Hydraulic Engineering* **125** (11), 1170–1180.

Lingireddy, S., Wood, D. J. & Zloczower, N. 2004 Pressure surges in pipeline systems resulting from air releases. *Journal (American Water Works Association)* **96** (7), 88–94.

Martin, C. S. 1976 Entrapped air in pipelines. In: *Proc., 2nd Int. Conf. on Pressure Surges.* British Hydromechanics Research Association, Bedford, UK, pp. 15–27.

Martin, C. & Lee, N. 2012 Measurement and rigid column analysis of expulsion of entrapped air from a horizontal pipe with an exit orifice. In: *Proceedings of the 11th International Conference on Pressure Surges*, pp. 527–542.

MATLAB 2015 *Version 8.6 (R2015b).* The MathWorks Inc., Natick, MA, USA.

Pozos-Estrada, O., Pothof, I., Fuentes-Mariles, O. A., Dominguez-Mora, R., Pedrozo-Acuña, A., Meli, R. & Peña, F. 2015 Failure of a drainage tunnel caused by an entrapped air pocket. *Urban Water Journal* **12** (6), 446–454.

Song, C. C., Cardie, J. A. & Leung, K. S. 1983 Transient mixed-flow models for storm sewers. *Journal of Hydraulic Engineering* **109** (11), 1487–1504.

Vasconcelos, J. G. & Wright, S. J. 2011 Geysering generated by large air pockets released through water-filled ventilation shafts. *Journal of Hydraulic Engineering* **137** (5), 543–555.

Wright, S. J., Lewis, J. W. & Vasconcelos, J. G. 2010 Geysering in rapidly filling storm-water tunnels. *Journal of Hydraulic Engineering* **137** (1), 112–115.

Wright, S. J., Lewis, J. W. & Vasconcelos, J. G. 2011 Physical processes resulting in geysers in rapidly filling storm-water tunnels. *Journal of Irrigation and Drainage Engineering* **137** (3), 199–202.

Wylie, E. B. & Streeter, V. L. 1978 *Fluid Transients*. McGraw-Hill International Book Co., New York, NY, USA.

Zhou, F., Hicks, F. E. & Steffler, P. M. 2002 Transient flow in a rapidly filling horizontal pipe containing trapped Air. *Journal of Hydraulic Engineering* **128** (6), 625–634.

Zhou, L., Liu, D., Karney, B. & Zhang, Q. 2011 Influence of entrapped air pockets on hydraulic transients in water pipelines. *Journal of Hydraulic Engineering* **137** (12), 1686–1692.

First received 14 December 2017; accepted in revised form 13 February 2018. Available online 23 February 2018